SCIENCE CHINA
Technological Sciences

• Article •

June 2015 Vol.58 No.6: 1096–1104
doi: 10.1007/s11431-015-5804-5

Preparation and characteristics of a recycled cement-based superhydrophobic coating with dirt pickup resistance

GUO LiPing[1,2,3*], SUN Wei[1,2,3], YU Tao[4] & FENG MuZai[5]

[1] *School of Materials Science and Engineering, Southeast University, Nanjing 211189, China;*
[2] *Collaborative Innovation Center for Advanced Civil Engineering Materials, Nanjing 211189, China;*
[3] *Jiangsu Key Laboratory of Construction Materials, Nanjing 211189, China;*
[4] *Wuxi Communication Engineering Co., Ltd., Wuxi 214026, China;*
[5] *Department of Civil, Environmental and Architectural Engineering, The University of Kansas, Lawrence, Kansas 66045, USA*

Received January 13, 2015; accepted March 20, 2015; published online April 15, 2015

We introduce a low-cost and effective technique that can transform waste cement-based dust into a superhydrophobic coating with dirt pickup resistance. An organic-inorganic hybrid superhydrophobic coating is prepared by the sol-gel method using methyltriethoxysilane as a precursor and waste cement-based dust as a film-forming material. Orthogonal experiments and a comprehensive scoring method were used to optimize the composition and production technologies. Our results show that this superhydrophobic organic-inorganic hybrid coating has an average static contact angle of 151.65° and low water adhesion. Related tests reveal that the dirt pickup resistance, washing resistance and film-substrate cohesion of this coating are also outstanding. The multi-scale physical and chemical mechanisms behind the properties of the coating are investigated. This recycled cement-based coating can be used as the external cover of engineering structures to protect them from corrosion.

recycled cement-based coating, superhydrophobicity, dirt pickup resistance, washing resistance, film-substrate cohesion, multi-scale mechanisms

Citation: Guo L P, Sun W, Yu T, et al. Preparation and characteristics of a recycled cement-based superhydrophobic coating with dirt pickup resistance. Sci China Tech Sci, 2015, 58: 1096–1104, doi: 10.1007/s11431-015-5804-5

1 Introduction

Coatings that are superhydrophobic and resist dirt pickup are an attractive approach to improve durability and extend the service life of structures by protecting them from issues such as snow or dirt sticking, contamination, and oxidation [1–6]. Hydrophobicity, also known as the *Lotus Effect*, which is named for the lotus plant, is a useful property for protective coatings [7–11]. The wettability of a solid surface is governed by both its physical and chemical properties. Generally, there are two ways to achieve superhydrophobicity: 1) via rough surfaces that are initially hydrophobic with a contact angle (CA) >90° and regular microscopic morphology, and 2) induce low surface free energy on the initially rough surface through modification or by applying a hydrophobic admixture [12]. There are many approaches to generate rough surfaces, for example, plasma polymerization/etching of polypropylene in the presence of polytetrafluoroethylene [13], microwave plasma-enhanced chemical vapor deposition, mixing a material capable of sublimation with silica or boehmite [5], molding [14], and phase separation [15]. In some cases, coating the surface with a low-surface-energy material like fluoroalkylsilane is needed to realize superhydrophobicity.

Solid waste from construction is becoming an increas-

*Corresponding author (email: guoliping691@163.com)

ingly serious problem, accounting for 30%–40% of all urban garbage [16]. Currently, 20% of China's GDP of 5.6 trillion Yuan is devoted to the construction industry, and the discharge of construction rubbish continues to increase with the acceleration of industrialization and urbanization. The annual output of the construction rubbish in China exceeds 300 million tons. Most of this material is left exposed to the weather or buried in rural areas without any treatment. Unfortunately, the dust particles with a diameter of less than 200 μm in this construction rubbish cause serious environmental pollution, and have been identified as the main cause of city smog. Based on these considerations, we decided that converting these tiny solid particles into superhydrophobic coatings with dirt pickup resistance coating would be a novel way to both recycle the waste and to decrease their environmental impact.

We selected waste cement-based concrete dust with a diameter of less than 200 μm as the recycled sample in this work, and investigated how such waste cement-based dust can be transformed into a sustainable recycled coating to protect buildings from dust. Carbon silicate hydrate gel (CSH gel) in waste concrete dust is a major hydration product of cement. To impart waste concrete with hydrophobicity, methyltriethoxysilane (MTES) can be used as a hydrophobic reagent to graft methyl groups onto the surface of CSH gel. MTES can hydrolyze methoxyl groups and generate silanol groups, and then the resulting silanol groups should react with the same groups on silica nanoparticles in the CSH gel to form Si-CH_3, which should make the waste cement powder superhydrophobic [17–20]. Coupling physical and chemical mechanisms together should an effective way to produce a novel coating using cement-based dust. In this study, we prepare a novel cement dust-based coating and investigate its ability to protect surfaces by measuring CAs of water, dirt pickup resistance, washing resistance and surface morphology.

2 Materials and methods

2.1 Raw materials

Waste cement-based paste collected from the demolition site of an old concrete building was ground before use. The resulting particle was characterized by a laser particle size analyzer, and ranged from 1.20 to 75 μm. The main components of the dust were unhydrated cement, calcium hydroxide and CSH gel. The surfaces of these particles were covered with hydroxyl groups (OH^-) when they were dispersed in water or anhydrous ethanol. MTES (98.0%, A.R. grade, MW=178.30 g/mol) and aqueous ammonia (NH_3, 25% in water, A.R. grade , MW=17.03 g/mol) were used as modification and curing agents, respectively. Anhydrous ethanol (C_2H_5OH, 99.7%, A.R. grade, MW=46.07 g/mol) was used as the solvent and dispersant.

2.2 Coating fabrication

The coatings were prepared by the sol-gel method. Briefly, the ground waste concrete dust was mixed with MTES and anhydrous ethanol and then heated at 50°C in a water bath while the mixture was also stirred by ultrasonication. NH_3 was added, and the mixture was kept at 50°C and ultrasonication for 30 min. The obtained suspension was diluted with distilled water and sprayed onto a thin mortar plate (80×40×12 mm) or glass slide at a distance of around 30 cm. The coating was then aged for 24 h at ambient temperature and pressure before characterization.

To optimize the composition of the reaction mixture, reaction conditions and production process, we investigated their effects on the superhydrophobicity of the obtained coatings through orthogonal tests, as shown in Table 1. Orthogonal tests considering of four factors and three levels ($L_9(3^4)$) were designed to investigate the influence of technical parameters on the CA of the coating. In the present study, the molar ratio of MTES to aqueous ammonia in the reaction solution was fixed at 1∶15.

The optimum number of sprayed layers of coating was determined. The mass of slurry with optimized composition sprayed on a thin mortar plate (50×30×10 mm) each time in this experiment was 0.15–0.2 g. After repeatedly spraying the coating material onto the substrate three, five or seven times, we air dried the samples for 24 h and then compared their macroscale appearance.

2.3 Characterization

CAs of the coating were evaluated by a CA test meter (OCA 20, Dataphysics, Stuttgart, Germany). Static contact angle (SCA) and contact angle hysteresis (CAH) measurements were also performed using the optical CA meter. The hydrophobicity of coatings was measured using water droplets with a volume of 5 μL. Each reported CA is the average of six CA measurements. CA hysteresis was measured by immobilizing the coated plate on a microscope base and tilting both the microscope and plate until the droplet rolled off the sample. The surface morphology of the coatings was measured by field-emission scanning electron microscopy (FESEM, Quanta 3D FEG, FEI Company, Eindhoven, the Netherlands). The surface roughness of the coatings was characterized by the contact mode of optical microscopy and atomic force microscopy (AFM, Dimension ICON, Bruker Corporation, New York, USA).

As well as superhydrophobicity, other important characteristics of the coatings were also investigated including dirt pickup resistance, washing resistance and film-substrate cohesion. To determine dirt pickup resistance, two test blocks (160×80×20 mm) with superhydrophobic coating were positioned at an angle of 10° from horizontal. Fly ash (50 g) was evenly sprinkled on one block, and then water (5 L) was poured over the blocks from a distance of 10 cm at a rate of around 1 L/min. The dirt pickup resistance was then

Table 1 Orthogonal test design

Test number	Factor			
	Mass fraction of dust (%)	[MTES] (mol/L)	[C_2H_5OH] (mol/L)	Reaction time (min)
1	17.0(I)	0.0082(I)	0.3479(I)	60(II)
2	17.0(I)	0.0125(III)	0.5220(III)	45(I)
3	17.0(I)	0.0104(II)	0.4350(II)	60(II)
4	25.5(II)	0.0084(I)	0.5220(III)	60(II)
5	25.5(II)	0.0125(III)	0.4350(II)	60(II)
6	25.5(II)	0.0104(II)	0.3479(I)	45(I)
7	17.0(I)	0.0082(I)	0.4350(II)	45(I)
8	17.0(I)	0.0125(III)	0.3479(I)	60(II)
9	17.0(I)	0.0104(II)	0.5220(III)	60(II)

evaluated through comparison of the two blocks. We also dried a test block (160×80×20 mm) until its weight was constant, and then evenly sprinkled fly ash (50 g) on its surface. The sample was weighed, tilted by 90°, weighed again, violently shaken, and then weighed. Washing resistance was examined according to GB/T 9780-2013 Test Methods for Dirt Resistance of Architectural Coatings. A concrete plate (30×30 mm) covered the coating was selected as the test sample. A small funnel was positioned a distance of 10 cm above the coating. Tap water was flowed through the funnel onto the sprayed coating for more than 24 h at a velocity of 1 L/h. Film-substrate cohesion was investigated by using a grid device to cut a 6×6 lattice of lines with a spacing of 2 mm on the coating. The lattice was cleaned with a dry brush along each diagonal direction five times, and further cleaned by tape-stripping once before being imaged by an optical microscope.

3 Results and discussion

3.1 Optimized composition of the reaction mixture

The results of the orthogonal tests are listed in Table 2. According to the results of variance analysis in Table 2, the greatest ranges appear in the columns that represent the content of anhydrous ethanol and MTES, which indicates that the amount of anhydrous ethanol and MTES are the two most important factors that influence the CA of the coatings. Changing the reaction time had relatively little effect on the CA of the coatings. Meanwhile, changes in the mass fraction of dust had a slightly greater influence than reaction time on CA, but the effect was still considerably less than those of MTES and ethanol.

If the mass fraction of waste cement-based dust is less than 25.5% of the total raw material, the CA of the coating is greater than 136°. When the mass fraction of dust is 17%, the maximum CA of the coating is 141.62°. This is possibly because an organic network begins to form when the content of waste cement-based dust is high enough, which enhances both the film formability and hydrophobicity of the coating. However, when the proportion of dust is too high, the steric hindrance is increased and the excess of gel starts to fill the rough structure of the coating. This leads to a high possibility of cracks forming on the coating surface. When the coating cracks, water can seep through it, and the CA is decreased.

The hydrolysate of MTES contains polar –OH and nonpolar $–CH_3$ groups. The $–CH_3$ groups can be chemically grafted onto the surface of the CSH gel, which can lead to hydrophobicity. The WCA of the coating increases to a peak value and then decreases as the content of anhydrous ethanol increases. Ethanol provides a homogeneous solution to facilitate hydrolysis between MTES and the CSH gel. The hydrolysates of ethanol are polar –OH and nonpolar $–CH_3CH_2$ groups, which can enhance the chemical stability of the MTES/CSH sol. As the amount of ethanol increases, the compatibility of the sol is strengthened and hydrophobicity is therefore enhanced. However, when the content of ethanol exceeds an upper limit, the chemical polarity of the sol-gel system becomes too strong and the hydrophobicity

Table 2 Results of orthogonal tests

Test number		Factor				Evaluation index
		Mass fraction of dust (%)	[MTES] (mol/L)	[C_2H_5OH] (mol/L)	Reaction time (min)	CA (°)
1		17.0(I)	0.0082(I)	0.3479(I)	60(II)	141.39
2		17.0(I)	0.0125(III)	0.5220(III)	45(I)	143.48
3		17.0(I)	0.0104(II)	0.4350(II)	60(II)	139.32
4		25.5(II)	0.0084(I)	0.5220(III)	60(II)	138.61
5		25.5(II)	0.0125(III)	0.4350(II)	60(II)	134.05
6		25.5(II)	0.0104(II)	0.3479(I)	45(I)	135.27
7		17.0(I)	0.0082(I)	0.4350(II)	45(I)	133.47
8		17.0(I)	0.0125(III)	0.3479(I)	60(II)	125.06
9		17.0(I)	0.0104(II)	0.5220(III)	60(II)	141.62
Average	I	137.39°	136.04°	130.16°	136.56°	
	II	135.98°	138.73°	135.61°	137.42°	
	III	–	134.20°	141.24°	–	
Range		1.41	4.53	11.08	0.86	

of the coating is weakened.

The effects of MTES content on CA are depicted in Figure 1(a). The CA of the coating increases from 136.04° to 138.73° as the MTES content is increased from 0.0082 to 0.0104 mol/L, but then starts to decrease when the content of MTES continues to increase. The effect of the content of anhydrous ethanol on the CA of the coatings is presented in Figure 1(b). CA increases with the content of ethanol, which indicates that with further increases in the content of anhydrous ethanol, the CA would continue to increase. However, we found that when the concentration of ethanol in the reaction mixture exceeded 0.522 mol/L, the number of cracks in the coating increased drastically, which decreased the CA.

Because we fixed the molar mass of aqueous ammonia to 15 times that of MTES in the present test, the optimized molar mass of aqueous ammonia could be determined after determining the optimized molar mass of MTES. Overall, it was concluded that the optimized ratio of raw materials was as follows: the optimal mass percentage of ground waste cement-based dust of the total raw material was 17%, and the optimal concentrations of MTES, anhydrous ethanol and ammonia were 0.0104, 0.5220 and 0.1560 mol/L, respectively. The optimum reaction time was 60 min at a temperature of 50°C.

The six CAs of coatings fabricated under the optimized conditions are 152.7°,152.8°, 151.8°, 151.9°, 150.4° and 150.3°. The average SCA was 152°, as shown in Figure 2, with a very limited CAH, which was determined as follows.

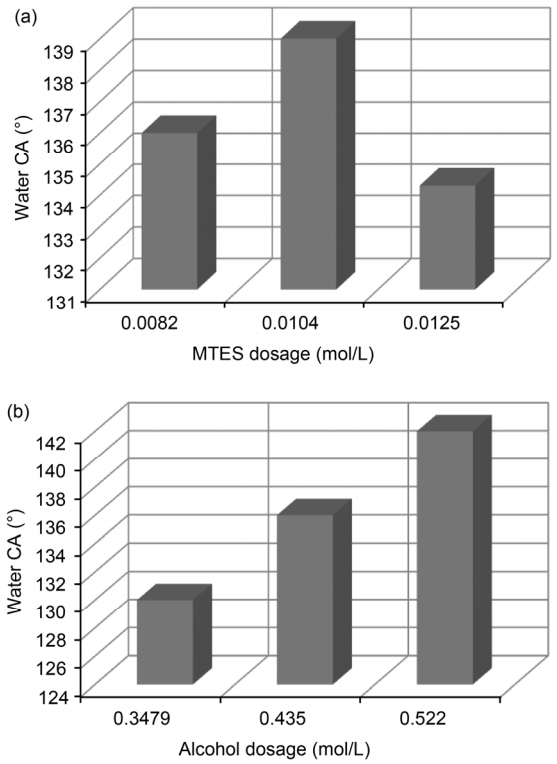

Figure 1 Effects of (a) MTES content, and (b) anhydrous ethanol content on the CA of the coatings.

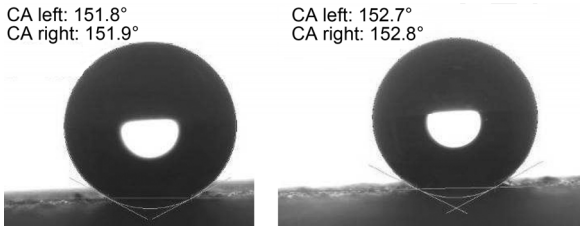

Figure 2 SCAs of water droplets on optimized coating surfaces.

A water droplet with a volume of 10 μL on the coating surface was lifted up at a rate of 0.5 cm/s by an injector pinhead, and then the CAH is the difference between the advancing contact angle (ACA) and receding contact angle (RCA). The process used to measure CAH is presented in Figure 3. A small CAH of 6.40° was obtained (Table 3), revealing that the recycled cement-based coating fabricated under optimized conditions is superhydrophobic.

3.2 Optimized number of sprayed layers

The number of layers sprayed, which equates to coating thickness, might also affect the multi-scale surface morphology and superhydrophobicity of the coatings. A coating that is too thick will easily crack on the surface, which allows water droplets to seep through and wet the substrate. Therefore, we sprayed coatings three, five, and seven times on the substrates. The results for the experiment investigating the optimum number of sprayed layers for the coating are shown in Figure 4. Figure 4(a) reveals that samples that were sprayed three times have level surfaces, without cracks (also see Figure 4(a)). In contrast the samples sprayed five times have surfaces with obvious spalling through which water can easily seep (Figure 4(b)). The samples that were sprayed seven times (Figure 4(c)) contained even larger fractures. Therefore, three sprayed layers produces an acceptable coating with a thickness of 150–200 μm.

3.3 Dirt pickup resistance

Because of its superhydrophobicity, the coating cannot be smeared with an aqueous solution of fly ash to test its resistance to dirt pickup, as described in GB/T 9780-2013 Test Methods for Dirt Resistance of Architectural Coatings. Instead, alternative approaches to investigate the dirt pickup resistance of the coating were used, including sprinkling fly ash onto dry samples and then either pouring water over the sample or shaking it at 90°. Photographs of the blocks following the experiment where water was poured over them are shown in Figure 5.

The results for the experiment where fly ash was sprinkled on a sample and then the sample was shaken at 90° are summarized in Table 4.

The dirt pickup resistance of the coating was evaluated according to eq. (1), wherein *DR* is the percentage of dirt

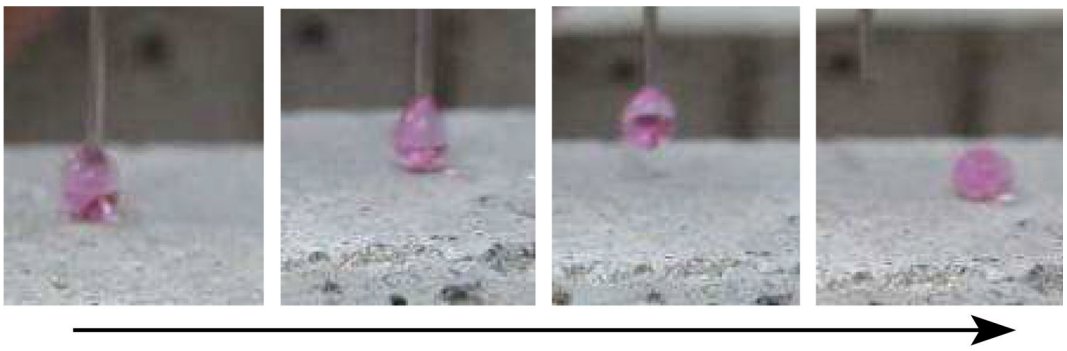

Figure 3 (Color online) Process used to measure CAH.

Table 3 SCAs of water droplets on optimized coating surfaces

Type of contact angle	SCA	ACA	RCA	CAH
Angle (°)	151.65	154.74	148.34	6.40

Figure 4 Macroscopic appearance of samples sprayed (a) three times, (b) five times, and (c) seven times.

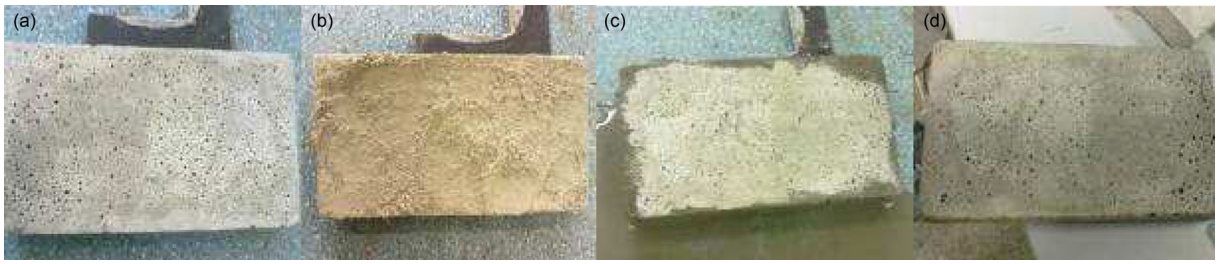

Figure 5 (Color online) Morphology of the block (a) before the experiment, (b) with fly ash, (c) after rinsing, and (d) after air-drying.

pickup resistance (%), m_0 is the original weight of the block with sprayed coating (g), m_2 is the final weight of the block after dust removal and oven drying (g).

$$DR = \left(1 - \frac{m_2 - m_0}{m_0}\right) \times 100\%. \quad (1)$$

3.4 Washing resistance

Considering the external surface of buildings is the main intended use of this coating, its washing resistance should be assessed to expand its engineering application. The washing actions of rain and cleaning will weaken the superhydrophobic performance of the coating. To confirm the stability of the coating, we evaluated the maximum number of washes it endure while maintaining optimized performance. Figures 6(a) and (b) reveal that the microstructures of the coating were not damaged by such washing and maintained their original state after washing for 96 h. Therefore, the coating has strong washing resistance.

Table 4 Evaluation of dirt pickup resistance of the coating

Original weight of block m_0 (g)	Weight of block and covered fly ash m_1 (g)	Final weight of block after cleaning m_2 (g)	Percentage of dirt pickup resistance DR (%)
450.12	500.14	450.15	99.3

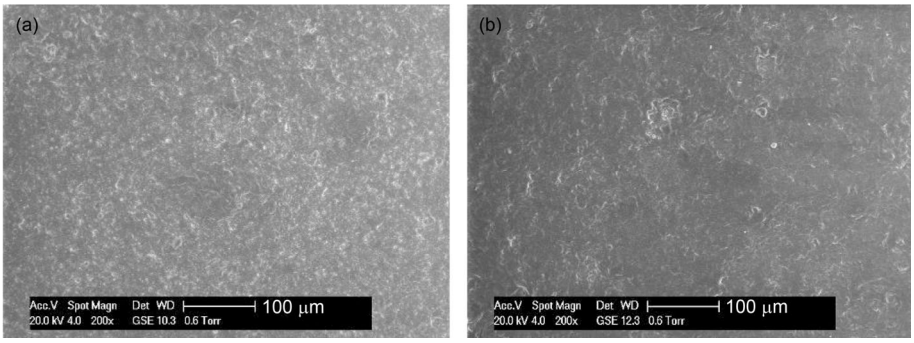

Figure 6 The morphology of a water drop on the coating surface (a) before and (b) washing with water.

3.5 Film-substrate cohesion

Normally the spalling and shedding of a coating from a substrate surface depend on debonding between the coating and substrate. The film-substrate attachment was investigated according to International Codes ISO2409 and ASTM D3359-B. If there are special requirements, the film-substrate cohesion must not be less than Class 1 according to ISO2409 or Class 4B according to ASTM D3359-B. The digital images of the lattice morphology captured by the CCD of a microscope are illustrated in Figure 7. Because the percentage of spalled area at the crossover points in this lattice was less than 5%, the film-substrate cohesion of the coating is Class 1 according to ISO2409 and Class 4B according to ASTM D3359-B. Therefore, the bonding of the coating to the substrate is strong enough to prevent shedding on the substrate.

3.6 Multi-scale physical morphology and chemical mechanism of the coating

The microscopic morphology and roughness of the coating were measured by FESEM, while its nanoscale morphology and roughness were characterized by AFM.

3.6.1 FESEM

After gold sputtering, the morphology of the coating was observed under vacuum by FESEM, as shown in Figure 8. The particles of the recycled concrete waste are tightly interconnected and there are no obvious cracks or voids found on the coating surface. These images reveal that the coating is made up of tiny platform-like particles with a uniform scale of about 5–10 μm (Figure 8(a)). There are also some flake-like $Ca(OH)_2$ crystals with size of about 5 μm (Figure 8(b)), which are a hydration product of cement. The coating is also covered by numerous spherical nanoscale cement hydrate particles (Figure 8(c)). These microscopic protuberances form a micro-nano structure on the coating surface, resembling a lotus leaf [9]. These results are predictable. This is because the CA of our coating is much larger than that of an ideal smooth surface modified with $-CH_3$, which is only about 110° [21]. It seems reasonable to infer that the superhydrophobicity of the coating is greatly increased by the presence of the nanoparticles.

Considering both the micro- and nanoscale structures in this coating, it actually contains two levels of uniform roughness. This kind of roughness is the main prerequisite to obtain superhydrophobicity. The optimized size distribution and uniform two-dimensional dispersion of recycled concrete particles are needed to realize the unique properties of this novel coating.

3.6.2 AFM

The nanoscale morphology of the coating surface was investigated by AFM in contact mode. The 3D images provide further evidence for the nanoscale roughness of the coating. Structures like spherical nanoparticles and flake-like matter are observed in Figures 9(a) and (b). Analysis of the AFM images using NanoScope image software revealed that the average roughness of the coating surface was

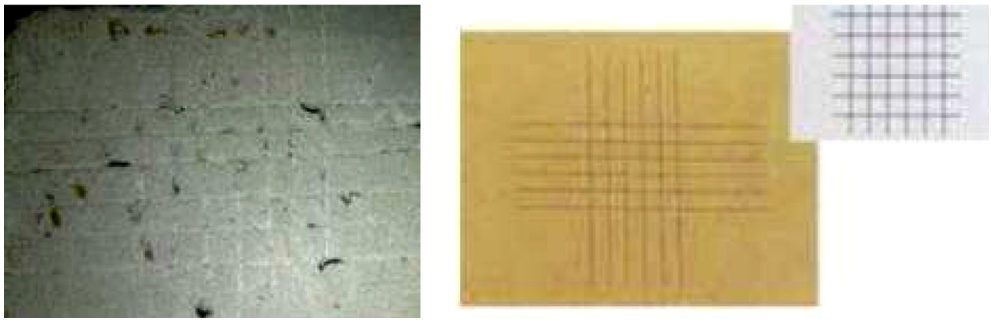

Figure 7 (Color online) Digital image and schematic diagram of the lattice used for the film-substrate cohesion test.

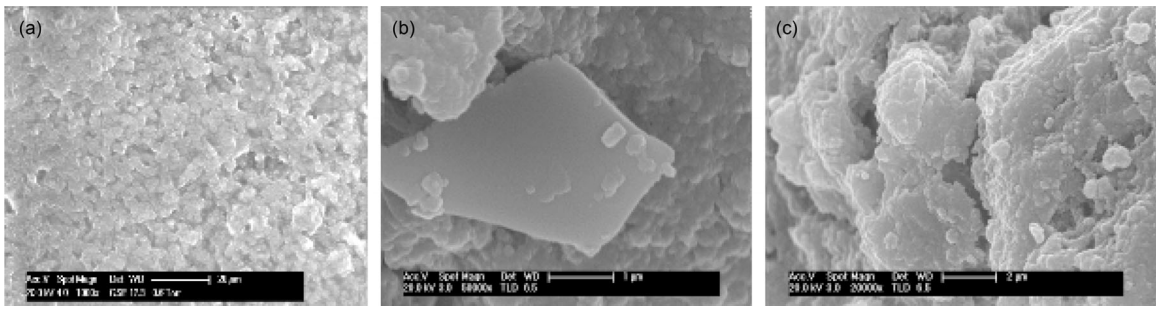

Figure 8 FESEM images of (a) overall topography, (b) plate-like structure, and (c) nanoscale structures of the coating.

around 1 μm, and the average space between particles was around 1 μm. Moreover, the particles were stably attached to each other throughout the organic superhydrophobic film. Overall, the results in Figures 8 and 9 indicate that the coating has a rough morphology with both micro- and nanoscale structures, which is similar to the structure of a lotus leaf. Therefore, we call this structure the "Pseudo-Lotus effect".

3.6.3 Chemical mechanism of superhydrophobicity

A superhydrophobic coating can be sustainably obtained by homogenizing multi-scale physical roughness. Low surface activity is also necessary to maintain long-term stability of superhydrophobicity [19]. CSH gel as the main hydrate of cement has a huge number of hydroxyl groups. If these hydroxyl groups are replaced by hydrophobic groups, the surface energy of the waste cement paste could be lowered. Now that we know the coating exhibits outstanding superhydrophobicity, it is important to determine the chemical groups grafted on the CSH gel particles. Infrared (IR) spectroscopy is an effective way to comprehensively evaluate the grafted chemical groups on the surface of CSH gels, so we measured the IR spectrum of the CSH gel (Figure 10). The major new active groups on the surface of the CSH gel are $-CH_3$ and $-CH_2$. By reducing the surface energy of the CSH gel, these grafted active groups are an inherent source of the superhydrophobicity and dirt pickup resistance of the coating.

3.6.4 Revised superhydrophobic model for the recycled cement-based coating

Based on the above-mentioned multi-scale physical-chemistry mechanisms that underpin the properties of the coating, a "Pseudo-Lotus Model", as shown in Figure 11, was developed to explain the superhydrophobicity of the recycled cement-based coating. This revised model is different from the Lotus and Gecko models [22]. The morphology of the rough surface was not uniform but contained multi-scale particles, which means that nanoparticles were nonuniformly adhered on the irregular microscale flakes and particles. In addition, decreasing the surface energy by chemical grafting of $-CH_3$ and $-CH_2-$ groups on the multi-scale particles could induce nanobubbles on their surfaces when in contact with water [23]. Therefore, multi-scale roughness and nanobubbles on the low-surface-energy particles endow this recycled cement-based coating with outstanding superhydrophobic and dirt-pickup-resistance characteristics.

4 Conclusions

A sol-gel method was used to recycle waste cement-based dust into a protective coating that was characterized by superhydrophobicity and dirt pickup resistance. We optimized

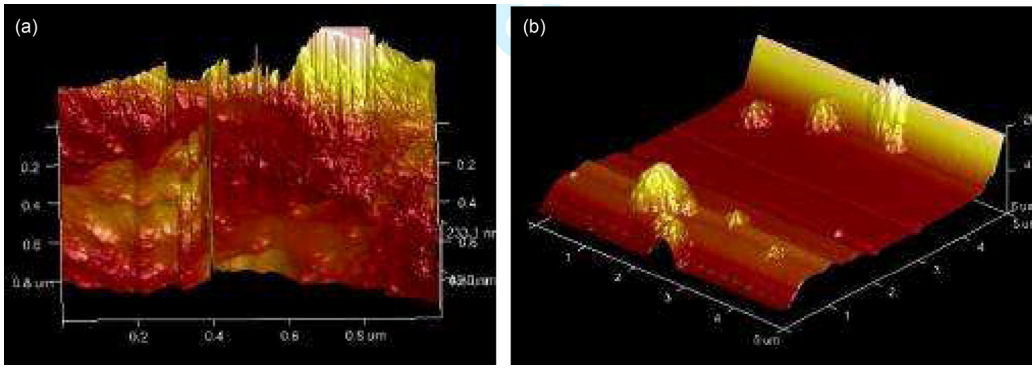

Figure 9 (Color online) AFM images of (a) 1×1 μm surface showing a platform-like structure and nanoparticles, and (b) 5×5 μm surface with flake-like matter and nanoparticles.

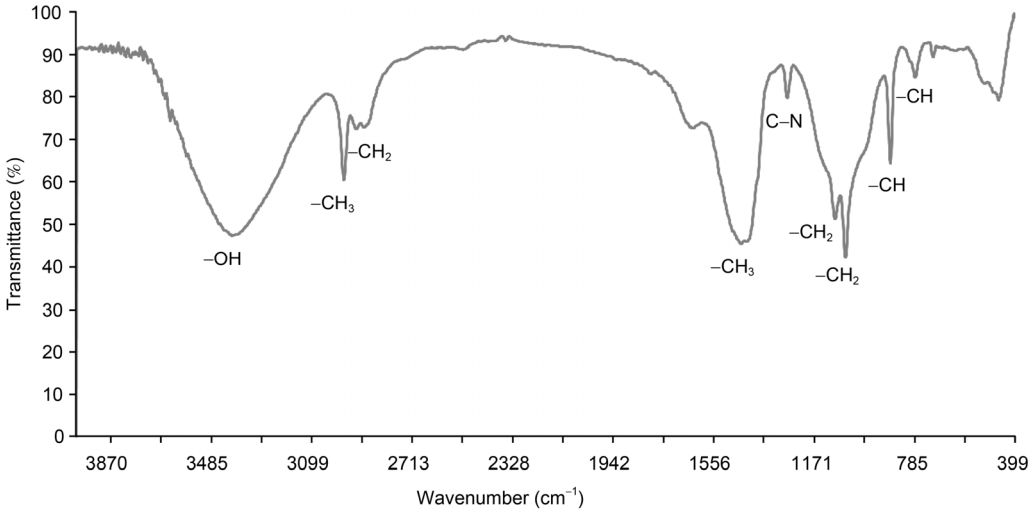

Figure 10 IR spectrum of the modified CSH gel.

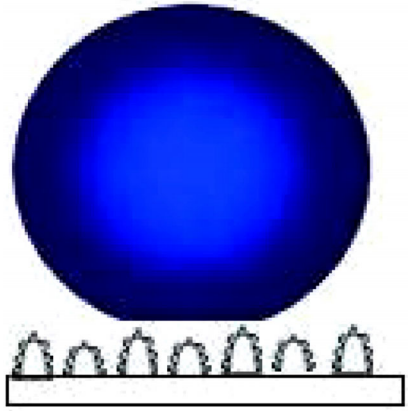

Figure 11 (Color online) Pseudo-lotus model of a superhydrophobic surface.

the mixture composition and production technology used to fabricate the coating by evaluating the effects of various factors on the CA of the coating. The microstructure and chemical composition of the coating are responsible for its superhydrophobicity and dirt pickup resistance. We found that rough nano-micro structures and grafted superhydrophobic chemical groups are two inherent origins of the superhydrophobicity and dirt pickup resistance of the coating. This novel coating is undoubtedly important for the protection of engineering structures from solution erosion and soiling caused by acid rain, seawater, saline soil solution, mill dust and haze.

This work was supported by the National Natural Science Foundation of China (Grant Nos. 51378113 and 51438003), and the National Basic Research Program of China ("973" Project) (Grant No. 2015CB655102).

1 Lee C, Kim C J. underwater restoration and retention of gases on superhydrophobic surfaces for drag reduction. Phys Rev Lett, 2011, 106: 014502
2 Yao X, Song Y L, Jiang L. Applications of bio-inspired special wettable surfaces. Adv Mater, 2011, 23: 719–734
3 Li Y, Li L, Sun J G. Bioinspired self-healing superhydrophobic coatings. Angew Chem Int Edit, 2010, 49: 6129–6133
4 Kulinich S A, Farhadi S, Nose K, et al. Superhydrophobic surfaces: Are they really ice-repellent? Langmuir, 2011, 27: 25–29
5 Nakajima A, Fujishima A, Hashimcto K, et al. Preparation of transparent superhydrophobic boehmite and silica films by sublimation of aluminum acetylacetonate. Adv Mater, 1999, 11: 1365–1368
6 Nahum T, Dodiuk H, Dotan A, et al. Superhydrophobic durable coating based on UV-photoreactive silica nanoparticles. J Appl Polym Sci, 2014, 131: 41122
7 Sun T, Feng L, Gao X, et al. Bioinspired surfaces with special wettability. Acc Chem Res, 2005, 38: 644
8 Gao L C, Fadeev A Y, McCarthy T J. Superhydrophobicity and contact-line issues. MRS Bull, 2008, 33: 747–751
9 Zhang J H, Sheng X L, Jiang L. The dewetting properties of lotus leaves. Langmuir, 2009, 25: 1371–1376.
10 Liu M J, Zheng Y M, Zhai J, et al. bioinspired super-antiwetting interfaces with special liquid-solid adhesion. Acc Chem Res, 2010, 43: 368–377
11 Manukyan G, Oh J M, van den Ende D, et al. Electrical switching of wetting states on superhydrophobic surfaces: A route towards reversible cassie-to-wenzel transitions. Phys Rev Lett, 2011, 106: 014501
12 Nosonosky M, Bhushan B. Artificial (Biomimetic) Superhydrophobic Surface. Multi-scale Dissipative Mechanisms and Hierarchical Surfaces: Friction, Superhydrophobicity, and Biomimetics. Heidelberg: Springer Press, 2008. 199
13 Chen W, Fadeev A Y, Heieh M C, et al. Ultrahydrophobic and ultralyophobic surfaces: Some comments and examples. Langmuir, 1999, 15: 3395–3399
14 Bico J, Marzolin C, Quere D. Pearl drops. Europhys Lett, 1999, 47: 220–226
15 Nakajima A, Abe K, Hashimoto K, et al. Preparation of hard super-hydrophobic films with visible light transmission. Thin Solid Films, 2000, 376: 140–143
16 Liang X Z, Wang H. Experimental research on roadway filling with skeleton type based on construction waste. Metal Mine, 2011, 11: 62
17 Yang H, Pi P H, Cai Z Q. Facile preparation of super-hydrophobic and super-oleophilic silica film on stainless steel mesh via sol-gel process. Appl Surf Sci, 2010, 256: 4095–4102
18 Latthe S S, Dhere S L, Kappenstein C, et al. Sliding behavior of water drops on sol-gel derived hydrophobic silica films. Appl Surf Sci, 2010, 256: 3259–3264

19 Latthe S S, Imai H, Ganesan V, et al. Porous superhydrophobic silica films by sol-gel process. Micropor Mesopor Mater, 2010, 130: 115–121
20 Liu X M, He J H. Superhydrophilic and antireflective properties of silica nanoparticle coatings fabricated via layer-by-layer assembly and postcalcination. J Phys Chem C, 2009, 113: 148–152
21 Fadeev A Y, McCarthy T J. Self-assembly is not the only reaction possible between alkyltrichlorosilanes and surfaces: Monomolecular and oligomeric covalently attached layers of dichloro- and trichloro-alkylsilanes on silicon. Langmuir, 2000, 16: 7268–7274
22 Hong X, Gao X, Jiang L. Application of superhydrophobic surface with high adhesive force in no lost transport of superparamagnetic microdroplet. J Am Chem Soc, 2007, 129: 1478–1479
23 Ishida N, Inoue T, Miyahara M, et al. Nanobubbles on a hydrophobic surface in water observed by tapping-mode atomic force microscopy. Langmuir, 2000, 16: 6377–6380